Journal of Magnetic Resonance 231 (2013) 133–140

Contents lists available at SciVerse ScienceDirect

Journal of Magnetic Resonance

journal homepage: www.elsevier.com/locate/jmr

Room temperature strong coupling between a microwave oscillator and an ensemble of electron spins

G. Boero [a,*], G. Gualco [a], R. Lisowski [a], J. Anders [a,c], D. Suter [b], J. Brugger [a]

[a] Ecole Polytechnique Federale de Lausanne (EPFL), CH-1015 Lausanne, Switzerland
[b] Technische Universität Dortmund, D-44221 Dortmund, Germany
[c] Universität Ulm, D-89069 Ulm, Germany

ARTICLE INFO

Article history:
Received 27 February 2013
Revised 5 April 2013
Available online 18 April 2013

Keywords:
EPR
Strong coupling
LC-oscillator

ABSTRACT

We demonstrate theoretically and experimentally the possibility to achieve the strong coupling regime at room temperature with a microwave electronic oscillator coupled with an ensemble of electron spins. The coupled system shows bistable behaviour, with a broad hysteresis and sharp transitions. The coupling strength and the hysteresis width can be adjusted through the number of spins in the ensemble, the temperature, and the microwave field strength.

1. Introduction

Achieving strong coupling between a microwave resonator and an ensemble of electron spins has become an important goal during the last years [1–14]. One of the motivations for these studies is the search for possible realizations of efficient quantum computers. The strength of the coupling between a resonator and an ensemble of electron spins is usually described by the collective coupling strength [2–5]. The collective coupling strength g_c can be expressed as $g_c = g_s\sqrt{N_p}$, where g_s is the cavity-single spin coupling strength, $N_p = N(\coth(\alpha) - (1/\alpha))$ is the equivalent number of polarized spins, $\alpha = \mu B_0/k_B T$, μ is the effective magnetic moment ($\mu = \mu_B\sqrt{3}$ for $S = 1/2$ and $g = 2$), B_0 is the static magnetic field, and N is the number of spins in the ensemble. A rough estimation of g_s is given by $g_s \cong \mu\sqrt{\mu_0\omega/2\hbar V_c}$ where V_c is the cavity volume, and ω is the transition angular frequency [2]. The strong coupling regime is usually identified by the conditions $g_c \gg \kappa, \gamma$, where κ and γ are the resonator and the spin resonance line half-width-at-half-maximum, both given in rad/s [2,4,5].

In contrast to previous work that described the coupling between a microwave *resonator* driven by an external microwave source and a spin ensemble [1–9,15,16], here we investigate theoretically and experimentally the coupling of a microwave *oscillator* and an ensemble of spins. In particular, we provide a simple theory describing the coupling of a microwave LC-oscillator with an ensemble of electron spins and we demonstrate experimentally that by this approach the strong coupling is observable also at room temperature. The strong coupling between the spin ensemble and the microwave oscillator leads to a cooperative behaviour of the combined system. The oscillation frequency of the coupled system shows a broad hysteresis and sharp transitions as a function of the applied static magnetic field. In the bistable region, the previous history of the system determines which of the two possible states is observed.

2. Theory

In typical experimental conditions, the oscillation frequency of an LC-oscillator coupled with an ensemble of electron spins is given by (see Appendix A)

$$\omega_{LC\chi} \cong \frac{\omega_{LC}}{\sqrt{1+\eta\chi'}}, \tag{1}$$

where

$$\chi' = -\frac{1}{2}\frac{(\omega_{LC\chi}-\omega_0)T_2^2}{1+T_2^2(\omega_{LC\chi}-\omega_0)^2+\gamma_e^2 B_1^2 T_1 T_2}\omega_0\chi_0, \tag{2}$$

$\omega_{LC} = 1/\sqrt{LC}$ is the unperturbed oscillator frequency, $\omega_0 = \gamma_e B_0$, χ_0 is the static susceptibility, η is the filling factor (approximately given by (V_s/V_c), where V_s is the sample volume), γ_e is the electron gyromagnetic ratio, B_1 is the microwave magnetic field, T_1 and T_2 are the relaxation times. Due to the dependence of χ' on $\omega_{LC\chi}$, Eq. (1) contains on both sides the oscillation frequency $\omega_{LC\chi}$. The determination of $\omega_{LC\chi}$ is equivalent to the determination of the roots of the function $F(\omega_{LC\chi}, B_0) = \omega_{LC\chi} - (\omega_{LC}/\sqrt{1+\eta\chi'})$ (or to the

* Corresponding author. Address: Ecole Polytechnique Fédérale de Lausanne (EPFL), BM-3-110, Station 17, CH-1015 Lausanne, Switzerland.
E-mail address: giovanni.boero@epfl.ch (G. Boero).

1090-7807/$ - see front matter © 2013 Elsevier Inc. All rights reserved.
http://dx.doi.org/10.1016/j.jmr.2013.04.004

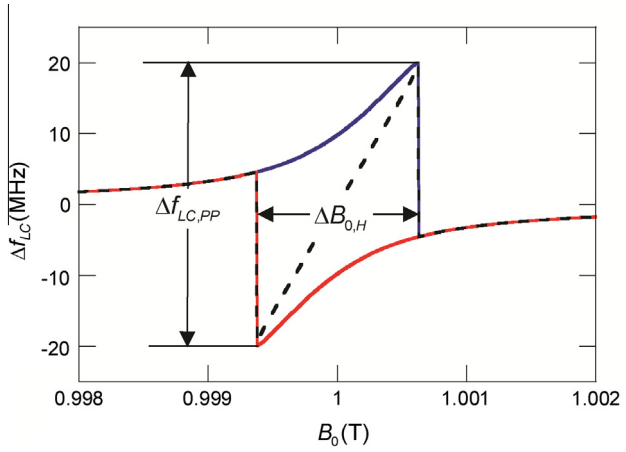

Fig. 1. Graphical representation of the three solutions for the oscillator frequency variation $\Delta f_{LC} = (\omega_{LC\chi} - \omega_{LC})/2\pi$ obtained solving Eq. (1). Simulation parameters: $T_1 = T_2 = 60$ ns, $\chi_0 = 5.2 \times 10^{-5}$, $f_{LC} = 28$ GHz, $\gamma_e/2\pi = 28$ GHz/T, $\eta = 0.01$, $B_1 = 0$. The static susceptibility is computed by the equation $\chi_0 = \mu_0 n \gamma_e^2 \hbar^2 / 4kT$ (which is valid for $S = 1/2$, $g = 2$, $\mu B_0 \ll kT$) assuming $T = 300$ K and $n = 2 \times 10^{27}$ spins/m^3. Relaxation times and spin density correspond to those of DPPH [17,18]. $\Delta f_{LC,PP}$ is the peak-to-peak oscillator frequency variation, $\Delta B_{0,H}$ is the hysteresis.

determination of the extrema of $U(\omega_{LC\chi}, B_0) = -\int F(\omega_{LC\chi}, B_0) d\omega_{LC\chi}$, which assumes the role of a pseudo potential).

We first discuss the solution of Eq. (1) in the limit of negligible saturation (i.e., for $\gamma_e^2 B_1^2 T_1 T_2 \ll 1$). As long as the coupling is weak (precisely for $(\eta\chi_0)^{1/2} T_2 \omega_0 < 2$), there is a single solution for $\omega_{LC\chi}$ for each value of B_0. For $(\eta\chi_0)^{1/2} T_2 \omega_0 \geqslant 2$, we find a single solution *far* from resonance and three solutions *close* to resonance. The condition $(\eta\chi_0)^{1/2} T_2 \omega_0 \geqslant 2$ is equivalent to the strong coupling condition $g_c \geqslant \gamma$ (see Appendix B). Fig. 1 shows an example of the solutions obtained in the conditions reported in the figure caption, which correspond to $(\eta\chi_0)^{1/2} T_2 \omega_0 \cong 8$. The curve plotted in blue corresponds to the curve experimentally observed when the magnetic field is swept from values well below resonance to higher values, whereas the curve in red[1] corresponds to the opposite sweep direction starting from a field value well above resonance. Due to the hysteresis, a sort of volatile memory is obtained. The solution plotted with a dashed line in black is not experimentally observed. This solution corresponds to a maximum of the pseudo potential U and it is given by $\omega_{LC\chi} = \omega_0$ within the hysteresis. If the oscillator is turned on with a magnetic field value within the hysteresis region, the solution in red is experimentally observed. This might be due to the relatively complex start-up mechanisms of the oscillations or to a not yet identified global energy minimum of the system (the pseudo potential has two local minima with the same pseudo energy).

The physical behaviour of the LC-oscillator coupled to the spin ensemble can be qualitatively explained as follows. If the field sweep is started from a field value below (above) the resonance conditions, the oscillator frequency $\omega_{LC\chi}$ is slightly above (below) the unloaded oscillator frequency ω_{LC} due to the negative (positive) susceptibility χ' (see Eq. (1)). If the magnetic field is swept towards higher (lower) values the oscillator frequency $\omega_{LC\chi}$ further increases (decreases) due to the change of the susceptibility. This is the reason why sweeping the field towards higher (lower) values the resonance condition is achieved for a field $B_0 \geqslant (\omega_{LC}/\gamma_e)$ ($B_0 \leqslant (\omega_{LC}/\gamma_e)$). The oscillator remains locked to the spin system even when the magnetic field has been increased (decreased) beyond the resonance condition for the uncoupled system $B_0 = (\omega_{LC}/\gamma_e)$.

[1] For interpretation of colour in Fig. 1, the reader is referred to the web version of this article.

Fig. 2a–d show the evolution of the oscillator frequency variation as a function of the static magnetic field for different values of the filling factor. For $\eta = 0.0001$ the frequency variation has a dispersion-like shape. For $\eta \geqslant 0.001$, which corresponds to $(\eta\chi_0)^{1/2} T_2 \omega_0 \geqslant 2$, a hysteresis together with sharp transitions appears. The abrupt frequency variations shown in Fig. 2b–d are infinitely sharp (i.e., a forbidden frequency band exists between the two allowed frequency values immediately before and after the transition). Fig. 2e shows the linear dependence of the oscillator frequency variation $\Delta f_{LC,PP}$ on the filling factor. The oscillator frequency variation is equal to $(1/8\pi)\omega_0^2 T_2 \eta\chi_0$, in the weak as well as in the strong coupling regime. Fig. 2e shows also that, for sufficiently large η, the width of the hysteresis $\Delta B_{0,H}$ is a linear function of the filling factor. For wide hystereses, the hysteresis width and the frequency variation are related by $\Delta B_{0,H} \cong \gamma_e 2\pi \Delta f_{LC,PP}$. Fig. 2f shows the slope of the oscillator frequency variation at resonance as a function of the filling factor. For small values of η, the slope grows linearly with the filling factor. Close to the onset of the hysteretic behaviour, the slope becomes orders of magnitude larger than the one predicted using a linear extrapolation from the slope at small filling factors. Fig. 2f shows also the field difference $\Delta B_{0,PP}$ between the extrema of the oscillator frequency variation. In the weak coupling limit, $\Delta B_{0,PP}$ corresponds to the resonance linewidth definition for a dispersion signal. In the strong coupling regime, $\Delta B_{0,PP} = \Delta B_{0,H}$. For η values just below the onset of the hysteresis, the dispersion signal is distorted and narrowed ($\Delta B_{0,PP}$ is reduced to half of its value in the weak coupling limit).

So far, we assumed negligible saturation of the spin system. Fig. 2g shows the oscillator frequency variation and the hysteresis width as a function of the microwave field strength. In the condition of negligible saturation, the oscillator frequency variation and the hysteresis width are approximately independent of B_1. In the condition of non-negligible saturation, the oscillator frequency variation as well as the hysteresis width decrease rapidly to zero.

3. Experiments

In order to experimentally verify the proposed simple theoretical model, we used a single-chip electron spin resonance detector similar to those we reported in [19,20]. Fig. 3 shows a photo and the block diagram of the realized chip, which essentially consists of two LC-oscillators operating at 20.6 GHz and 17.1 GHz, respectively. The excitation/detection octagonal coils have a diameter of 200 μm, an inductance of 300 pH, a resistance of 2 Ω, and a Q-factor of 20. The microwave magnetic field B_1 can be varied from 0.1 to 0.7 mT by changing the oscillator supply voltage from 0.5 to 3.5 V. On the same chip, a mixer and a frequency division stage are also integrated. By mixing the two oscillator output voltages a signal at about 3.5 GHz is obtained, which is subsequently divided by 16, resulting in a chip output signal at about 220 MHz. The output frequency is measured with a frequency counter as a function of the applied static magnetic field B_0. The experimental oscillator linewidth is $\kappa \cong 2 \times 10^4$ rad/s, as measured by the virtual damping rate method [21]. Due to a relatively large $1/f^3$ component in the oscillator phase noise [22], the measured κ is two orders of magnitude larger than the thermal noise limited value, with an experimental linewidth compression of about 5×10^{-6} (see Appendix C).

The experiments reported in Fig. 4 are performed with a sample of DPPH having a volume of about $90 \times 90 \times 50\ \mu m^3$ and $T_2 \cong 56$ ns at 300 K as well as 77 K (see Appendix D). At 300 K, from the description of our experimental conditions reported above, we have $g_c \cong 2 \times 10^8$ rad/s, $\gamma \cong 2 \times 10^7$ rad/s, and $\kappa \cong 2 \times 10^4$ rad/s. Consequently, the strong coupling conditions $g_c \gg \gamma, \kappa$ are fulfilled. Fig. 4a reports measurements performed to experimentally dem-